Contribution of zooplankton fecal pellets to deep ocean particle flux in the Sargasso Sea assessed using quantitative image analysis

Article *in* Journal of Plankton Research · August 2012

DOI: 10.1093/plankt/fbs053

CITATIONS
15

READS
164

4 authors, including:

Olga Shatova
University of Otago
9 PUBLICATIONS **81** CITATIONS

SEE PROFILE

David A. Koweek
Carnegie Institution for Science
34 PUBLICATIONS **322** CITATIONS

SEE PROFILE

JOURNAL OF PLANKTON RESEARCH | VOLUME 34 | NUMBER 10 | PAGES 905–921 | 2012

Contribution of zooplankton fecal pellets to deep ocean particle flux in the Sargasso Sea assessed using quantitative image analysis

OLGA SHATOVA[1†], DAVID KOWEEK[2‡], MAUREEN H. CONTE[1,2*] AND JOHN C. WEBER[2]

[1]BERMUDA INSTITUTE OF OCEAN SCIENCES, FERRY REACH, ST GEORGES GE01, BERMUDA AND [2]ECOSYSTEMS CENTER, MBL, WOODS HOLE, MA 02543, USA

[†]PRESENT ADDRESS: DEPARTMENT OF MARINE SCIENCE, UNIVERSITY OF OTAGO, DUNEDIN 9054, NEW ZEALAND

[‡]PRESENT ADDRESS: DEPARTMENT OF ENVIRONMENTAL EARTH SYSTEMS SCIENCE, STANFORD UNIVERSITY, STANFORD, CA 94305, USA

*CORRESPONDING AUTHOR: mconte@mbl.edu

Received February 6, 2012; accepted in principle June 18, 2012; accepted for publication June 22, 2012

Corresponding editor: Roger Harris

Fecal pellet flux and size distribution at 500, 1500 and 3200 m depths were measured in sediment trap samples collected by the Oceanic Flux Program time-series off Bermuda, December 2006–November 2007. During the study, three mesoscale eddies passed through: a cyclonic eddy in bloom stage (February through mid-April), a decaying post-bloom mode-water eddy (late April through May), and an anticyclonic eddy (August through October). Variability associated with eddy passage masked any seasonal trends in flux or size distributions. At a depth of 1500 m, the fecal pellet flux ranged from a minimum of 100 pellets m^{-2} day^{-1} to a maximum of 500 pellets m^{-2} day^{-1} during the cyclonic eddy passage, corresponding to ranges in the fecal pellet mass and the carbon flux of 0.5–1.7 mg m^{-2} day^{-1} and 0.07–0.25 mg C m^{-2} day^{-1}, respectively. Fecal pellets averaged 7 $\pm$ 3% of the organic carbon flux, a minimum estimate as disassociated pellets were not quantifiable. Size distribution shifts indicated small zooplankton and immature stages were more abundant within the cyclonic eddy, whereas larger zooplankton were present within the mode water and anticyclonic eddies. The fecal pellet number, flux and size distributions showed no consistent depth trends and indicated extensive fecal pellet reprocessing within the water column.

KEYWORDS: fecal pellets; particle flux; zooplankton; Oceanic Flux Program; Sargasso Sea

INTRODUCTION

The oceanic particle flux is an essential component of the global carbon, nutrient and elemental cycles and transports both biogenic and lithogenic material to the deep ocean (reviewed in Honjo *et al.*, 2008). Organic components of the particle flux, for example phytoplankton cells, zooplankton fecal pellets, detritus and "marine snow" or amorphous aggregates, also carry reduced carbon compounds to depth, supporting deep ocean ecosystem metabolism (e.g. Alldredge, 2001; Gooday, 2002; Yamaguchi *et al.*, 2002). Temporal variability of particle fluxes depends upon the seasonal cycle of primary and secondary production as well as non-seasonal physical forcing (e.g. passage of weather

doi:10.1093/plankt/fbs053, available online at www.plankt.oxfordjournals.org. Advance Access publication July 23, 2012

systems and mesoscale physical features) and is modulated by biological processes within the water column (e.g. Angel, 1989; Lampitt and Antia, 1997; Conte *et al.*, 2001, 2003; reviewed in Honjo *et al.*, 2008). Subtle changes in the complex of physical and biological interactions that control particle production and particle recycling in the water column can have a large effect on the transfer efficiency of the biological pump. Thus, better knowledge of these interactions is a key to understanding the role of the oceanic particle flux in global carbon and elemental cycles and to predicting the consequences of changes in marine ecosystems due to climate change.

Zooplankton fecal pellets are a ubiquitous component of the oceanic particle flux and are an important nutrient source for deep water ecosystems (reviewed in Turner, 2002). The transfer efficiency of the fecal pellet flux depends upon pellet sinking rates, which are a function of pellet size and density, as well as the extent of pellet consumption and recycling in the water column (Small *et al.*, 1979; Angel, 1989; Lampitt *et al.*, 1990; Wassmann, 1998; Wexels Riser *et al.*, 2001, 2002). Small pellets are likely to be important for recycling of organics in the water column, whereas large pellets that sink faster are more efficient for the transport of organic material to depth (Wassmann, 1998). Within the water column, fecal pellets experience microbial degradation, re-ingestion by zooplankton (coprophagy) and fragmentation (coprohexy) via sloppy feeding that leads to the formation of small slowly sinking particles (Smetacek, 1980; Noji *et al.*, 1991; Gonzalez and Smetacek, 1994; Wilson *et al.*, 2008). Small fecal pellets may, in turn, be consumed by mesozooplankton that produce larger pellets, enhancing the transfer efficiency of the biological pump.

Microscopic analyses of fecal pellets collected in sediment traps have found great variability in size, shape and color as well as changes in the distribution and types of fecal pellets with depth indicating extensive recycling and reprocessing of fecal pellets by deep-dwelling zooplankton communities (Urrère and Knauer, 1981; Pilskaln and Honjo, 1987; Youngbluth *et al.*, 1989; Noji *et al.*, 1991; Carroll *et al.*, 1998; Gonzalez *et al.*, 2000; Wilson *et al.*, 2008). Although microscopic studies have provided a wealth of information on the fecal pellet flux, fecal pellet analysis using manual methods is extremely time-consuming and involves errors of human subjectivity. Automated image analysis of quantitative microphotographs of sediment trap contents enables a much more extensive data set to be generated than is possible using manual methods. Additionally, image analysis is non-destructive and requires no physical manipulation and so sample integrity is preserved.

Here, we used quantitative image analysis to study temporal variations in the fecal pellet flux and size distributions in the northern Sargasso Sea near Bermuda. We enumerated fecal pellets in the 500, 1500 and 3200 m sediment traps collected by the Oceanic Flux Program time-series (OFP, Conte *et al.*, 2001). The period of study (December 2006–November 2007) was marked by the passage of three mesoscale eddies: a cyclonic eddy with a developing phytoplankton bloom (February–April), a mode-water eddy in the post-bloom status (late April–late May) and a strong and intensifying anticyclonic eddy (late August–October). The passage of these different eddies provided an excellent natural laboratory to investigate how upper ocean physical forcing affects biogeochemical properties and zooplankton communities in surface waters, in turn affecting the fecal pellet flux at mesopelagic and bathypelagic depths.

Study area

The Bermuda Time-Series Site, located in the northern Sargasso Sea, is one of the most extensively studied open ocean regions and the site of several ongoing, complementary time-series: the Hydrostation S time-series (32°10′N, 64°30′W) of 0–2600 m hydrographic properties (Michaels and Knap, 1996), the Oceanic Flux Program (OFP) time-series (31°50′N, 64°10′W) of the deep ocean particle flux (Conte *et al.*, 2001), the Bermuda Atlantic Time-Series Study (BATS) time-series of upper ocean biogeochemistry (Steinberg *et al.*, 2001) and the Bermuda Testbed Mooring (BTM, 1994–2007) time-series of meteorological, physical and optical properties in the 0–650 m water column (Dickey *et al.*, 2001). Together with remote sensing, these time-series provide a uniquely detailed view of the complex interactions among physics, chemistry and biology in the oligotrophic North Atlantic gyre.

The seasonal cycle at Bermuda has been previously described (Michaels and Knap, 1996; Steinberg *et al.*, 2001). The mixed layer reaches a maximum depth of 250–300 m in late winter. With the onset of seasonal stratification in late February– early March, a short spring bloom develops and phytoplankton biomass and particulate organic carbon (POC) and nitrogen reach maximum concentrations. As seasonal stratification intensifies, a shallow, nutrient-depleted surface mixed layer develops with a subsurface chlorophyll

maximum at the base of the mixed layer. Strong thermal stratification in summer and autumn results in low vertical mixing that limits nutrient availability and primary production. Seasonal cooling in late autumn leads to gradual mixed layer deepening, renewed nutrient entrainment into the euphotic zone and increased productivity.

The seasonal zooplankton cycle features a biomass maximum in spring which is typically about three times higher than that of late summer (Deevey and Brooks, 1977; Madin *et al.*, 2001). Large zooplankton tend to be more abundant in spring while smaller zooplankton are more abundant in summer (Roman *et al.*, 1995). This suggests that macrozooplankton are more efficient grazers of the large phytoplankton typical of the spring bloom, whereas small zooplankton are more efficient grazers on the picoplankton typical of summer. Non-seasonal variability in the zooplankton biomass is also present, especially in autumn and winter (Madin *et al.*, 2001). There is a weak correlation between the zooplankton biomass and export carbon flux measured by drifting traps (Madin *et al.*, 2001).

Deep particle flux follows the seasonal production cycle, with a maximum in early March and a secondary maximum in late December—early January in some years (Conte *et al.*, 2001). Averaged over the 20 years of data (1989–2009), the 1500 m mass flux varies annually by a factor of three, from 24.4 mg m^{-2} day^{-1} in early October to 64.7 mg m^{-2} day^{-1} in early March. Significant inter-annual variability, as well as episodic and non-seasonal flux variability, is present (Conte *et al.*, 1998, 2003).

Much of the non-seasonal variability in the Sargasso Sea has been attributed to physical forcing such as the passage of synoptic-scale weather systems and mesoscale features such as eddies (e.g. Dickey *et al.*, 2001; Conte *et al.*, 2003; Sweeny *et al.*, 2003; Goldthwait and Steinberg, 2008; Krause *et al.*, 2010). Cyclonic and mode water eddy circulation elevates the pycnocline, enhancing nutrient upwelling and, in turn, phytoplankton production (McGillicuddy and Robinson, 1997; McGillicuddy *et al.*, 1999; Siegel *et al.*, 1999; Ledwell *et al.*, 2008). The physical structure of mesoscale features may also perturb vertical mixing and nutrient influx into the euphotic zone, leading to transient peaks in production and export flux (Conte *et al.*, 2003). Upwelling of nutrient-enriched waters at anticyclonic eddy frontal boundaries can locally stimulate phytoplankton production as well as promote localized physical aggregation of zooplankton, (Hernández-Leon *et al.*, 2001; Mackas *et al.*, 2005; Yebra *et al.*, 2004, 2005).

METHOD

Sediment trap methodology, sample collection and processing.

The OFP mooring and sample collection protocols are detailed in Conte *et al.* (Conte *et al.*, 2001). McLane Parflux sediment traps (0.5 m^2 surface area; McLane Labs, Falmouth, MA, USA) are positioned at 500, 1500 and 3200 m depths. The traps are programmed at ~2-week sampling resolution. Sample cups are filled with high-purity seawater brine (~40 ppt) that is prepared by freezing Sargasso Sea deep water (3000 m depth). The brine is poisoned with ultra-high purity $HgCl_2$ (200 mg L^{-1}) to arrest biological degradation during sample collection.

OFP sample processing and analytical protocols have been previously described (Conte *et al.*, 2001, 2003; Huang and Conte, 2009). The >1 mm-sized material (which interferes with quantitative splitting) is removed by gentle sieving prior to sample splitting and transferred to a pre-weighed Petri dish for swimmer removal and photography. The remaining <1 mm material is split into 10 subsamples using a McLane rotary sample splitter (McLane Labs, Falmouth, MA, USA). Four subsamples are removed for trace elemental and organic studies. The remaining subsamples (60%) are recombined and size fractionated into 500–1000, 125–500 and <125 μm size fractions. Each fraction is gently transferred to pre-weighed Petri dishes for quantitative photography (described below). After photography, the samples are dried at 60°C, weighed to the nearest 0.01 mg and transferred to 4 mL vials with Teflon-lined caps for archiving. Organic carbon and nitrogen concentration and isotopic composition are measured on 3–4 mg subsamples using a Europa 20-20 CF-IRMS mass spectrometer interfaced to a Europa ANCA-SL elemental analyzer, after sample acidification with H_2SO_3 to remove carbonates.

Image acquisition and analysis

The >1 mm, 500–1000 μm and 125–500 μm fractions are quantitatively photographed immediately after splitting using a Zeiss Stemi SV-11 stereomicroscope in conjunction with an Olympus Q-Color 5 (5.0 MP) camera. The Petri dish containing the sample in liquid is placed on a 1 cm^2 gridded photographic template that sits on blue optical flat glass (Schott IMERA 4218, Schott USA), a color that reduces refraction and provides optimal contrast of both light and dark particles. A fiber-optic ring light and a 10 × 12 cm back light fitted with a blue dichroic in-line filter (Schott A09070/A08931) are used to eliminate shadowing. The sample is gently distributed in the dish, and then each grid is

photographed. Magnification, photographic and illumination settings are tightly controlled to maintain image uniformity within and between sets of sample microphotographs.

The digital microphotographs for each sample (69 images total) were analyzed using Axiovision image analysis software (v.4.8.0, Carl Zeiss Imaging, Inc.). An empirically optimized automatic measurement algorithm was developed to identify and size the fecal pellets. The algorithm first separates the fecal pellets from the rest of the image matrix using a combination of RGB color channel and size criteria, and then tabulates the size, shape and color for each fecal pellet identified within the image (Fig. 1a and b). Results were edited post-processing to remove false-positive identifications. Between 370 and 3524 pellets were measured in each sample.

Fecal pellet volume was calculated using Axiovision parameters of the length (ellipse major radius) and width (ellipse minor radius) (Fig. 1c). As observed elsewhere (reviewed in Turner, 2002), fecal pellets in the traps were predominately cylindrical, elliptical and near-spherical particles. We approximated fecal pellet geometry as an ellipsoid:

$$V = \left(\frac{4}{3}\right)\pi ab^2,$$

where a and b are the radii of the ellipse major radius and ellipse minor radius, respectively. We limited our analysis to the 125–500-μm size fraction as the larger size fractions contain very few fecal pellets (infrequently an euphausiid fecal string). Very small pellets and disaggregated fecal material in the <125-μm size fraction cannot be enumerated using this method. Thus, our results are a conservative estimate of the total contribution of fecal material to the particle flux.

In addition to fecal pellets, we estimated the flux of amorphous aggregates by summing the aggregates in the 125–500, 500–1000 and >1000 μm size fractions (Fang *et al.*, 2010). The perimeter of each aggregate was manually outlined using the Axiovision software drawing tool. The area of each aggregate as well as the total area of aggregates in the image was then computed. Because fragile aggregates are likely to break apart during processing, we considered only the total aggregate area. As with fecal pellet data, our aggregate flux estimates do not include material in the <125-μm size fraction.

The fecal pellet volume was converted to a dry mass using Ploug *et al.* (Ploug *et al.*, 2008) estimate of the copepod fecal pellet specific dry weight density (0.55 gdw cm^{-3}). This value is only approximate, as there are few data on specific dry weight density of fecal pellets. The carbon content of fecal pellets at mesopelagic depths is also poorly known, and furthermore can vary significantly depending upon the food concentration and composition (e.g. Urban-Rich *et al.*, 1998; Atkinson *et al.*, 2012). As a first-order estimate, we used 0.08 mg C mm^{-3}, which is in the middle of the range of values reported for brown copepod fecal pellets in

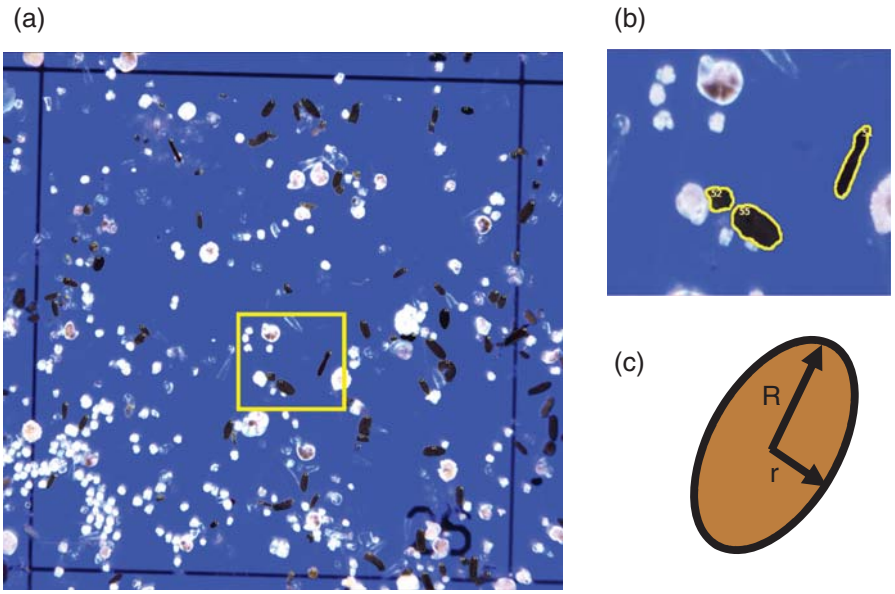

Fig. 1. (**a**) Typical microphotograph of a 1 cm^2 sample grid showing results of image analysis processing. (**b**) A magnification of the section of the grid highlighted in (a). The fecal pellet edge determined by the algorithm is outlined. (**c**) A cartoon of the idealized ellipsoid pellet shape showing the ellipse major (R) and minor (r) radii used to convert pellet area to volume.

the oligotrophic surface waters in the Arabian Sea (Urban-Rich *et al.*, 1998) and in the Humbolt Current off Chile (Gonzalez *et al.*, 2000). This estimate is slightly lower than that of freshly produced fecal pellets (0.11 mg C mm^{-3}) from surface-dwelling copepods collected in the northwest Mediterranean Sea (Carroll *et al.*, 1998), but higher than that in pellets produced by subpolar zooplankton (0.016–0.061 mg C mm^{-3}, Gonzalez *et al.*, 1994)

To convert the aggregate area to (dry) mass flux, we estimated the average aggregate thickness in the sample dish as 50 μm, based on the microscopic depth of field. We assumed an aggregate density contrast of Δρ of 1.01 (Jackson and Checkley, 2011), giving an approximate aggregate wet weight density of 0.104 g cm^{-3}, and assumed an average aggregate porosity of 90%. While only a rough first-order estimate of the aggregate mass flux, the uniform aggregate morphology observed in samples suggests that these estimates are internally consistent and thus have minimal temporal bias over the study period. Given the sparse data on the aggregate carbon content, we did not attempt to estimate the aggregate carbon flux.

Other data sets

Satellite data on the sea level anomaly (SLA) and MODIS ocean chlorophyll concentration during the study period were obtained from the Colorado Center for Astrodynamics Research (CCAR). *In situ* monthly data on upper ocean physical and biological parameters measured at the nearby BATS site was obtained from the BATS database. Additional unpublished data on *in situ* temperature and acoustic doppler current profiler (ADCP) current and backscatter data measured by sensors on the BTM was provided courtesy of T. D. Dickey, BTM principal investigator. Methods employed by the BATS time-series program are described in Steinberg *et al.* (Steinberg *et al.*, 2001). Methods employed by the BTM program are described in Dickey *et al.* (Dickey *et al.*, 2001) and Jiang *et al.* (Jiang *et al.*, 2007).

RESULTS

Mesoscale eddies and upper ocean biogeochemical variability during 2007

Satellite data on the SLA and chlorophyll and *in situ* data collected by the BTM Mooring (Smeti *et al.*, 2010) show the passage of three eddies across the Bermuda Time Series Site in 2007. A strong cyclonic eddy (Eddy C) with a negative SLA of <-25 cm formed east of the site in late winter (Fig. 2). As Eddy C propagated westward through the site between January and mid-April, a phytoplankton bloom was developing. Surface chlorophyll concentrations doubled in the eddy center, with

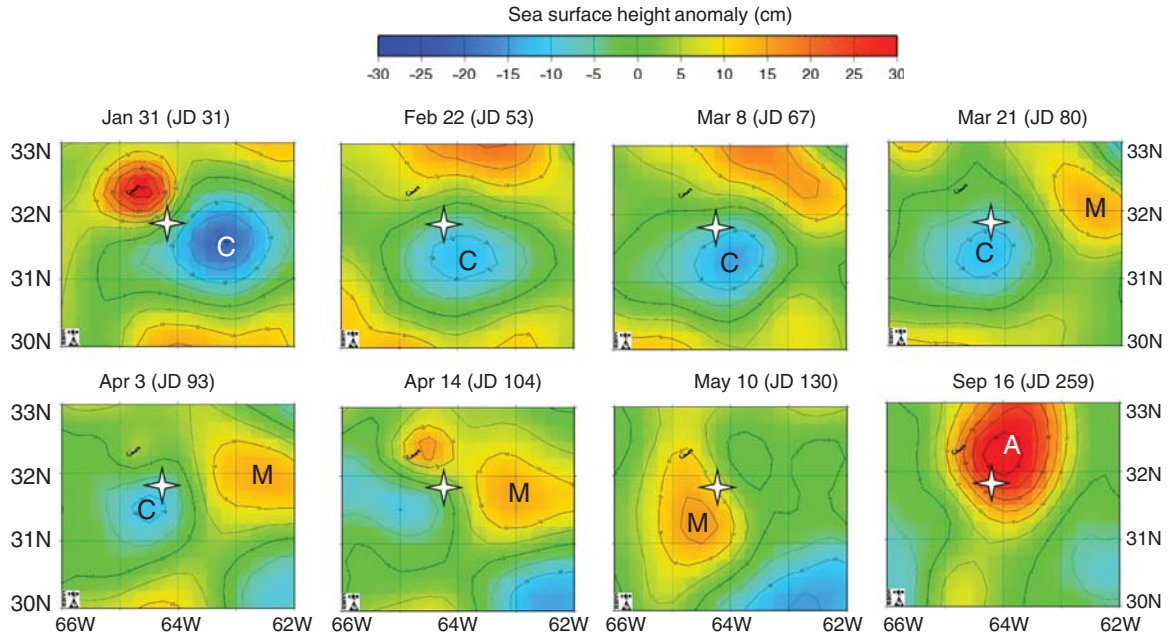

Fig. 2. Maps of the sea level anomaly (SLA) derived from satellite altimeter data for time periods when mesoscale eddies passed through the Bermuda Time Series area in 2007. SLA maps generated by Colorado Center of Astrodynamics Research. The star indicates the location of the OFP mooring (31°50′N, 64°10′W). The maps show the cyclonic (C), mode water (M) and anticyclonic (A) eddies near the dates when upper ocean measurements were taken by the BATS program (Fig. 3).

elevated chlorophyll near the eddy periphery (Smeti *et al.*, 2010). The mixed layer deepened to roughly 160 m of depth as Eddy C passed over the BATS site between Julian Day (JD) 29 and JD 67 (Fig. 3a). As the bloom developed in Eddy C, mixed layer Chl *a* concentrations rose from ~250 ng kg^{-1} (JD 29) to 300 ng kg^{-1} (JD 54) and mixed layer nitrite and nitrate concentrations decreased from 0.5 μmol kg^{-1} to 0.2 μmol kg^{-1} (Fig. 3b and c) Chl *a* concentrations decreased slightly to 200 ng kg^{-1} as the eddy center passed over (JD 67), but then increased again to 300 ng kg^{-1} in the eddy periphery (JD 93), consistent with satellite data that indicated the highest phytoplankton biomass at the eddy periphery. The 0 – 200 m daytime zooplankton biomass also doubled as Eddy C passed through the site (Fig. 3d). As Eddy C passed through its eddy circulation was weakening and shortly afterward was barely discernible from its SLA (Fig. 2).

Just behind Eddy C was a weakening mode water eddy (Eddy M), which had formed northeast of the site in early March (Fig 2, JD 130). Krause *et al.* (Krause *et al.*, 2010) sampled in Eddy M in April (JD 109 and JD 115). At the time of their sampling, there was a strong bloom in the eddy center that was dominated by large diatoms such as *Chaetoceros* sp. Biogenic silica concentrations and production rates within Eddy M were six times higher than in the surrounding waters. However, by early May (JD 138), Eddy M had a shallow nutrient-depleted mixed layer and low phytoplankton biomass with a weak subsurface chlorophyll maximum. These data confirmed the post-bloom status of Eddy M as it passed through the site. Shortly thereafter, Eddy M was no longer detectable from its SLA. The zooplankton 0–200 m biomass remained elevated in the transition zone between Eddy C and Eddy M (JD 104). Although no tows were made within the center of the Eddy M, the nighttime zooplankton biomass in the eddy periphery on JD 132 (650 ± 1 mg m^{-2}) was only 60% of that in Eddy C.

In late August and September a strong anticyclonic eddy (Eddy A), which had formed in early August, passed just north of the site. At its closest approach (Fig 2, JD 259), Eddy A was intensifying with a SLA of > 30 cm. The nighttime zooplankton biomass in the upper 200 m in the frontal boundary of Eddy A (JD 244) was approximately twice that observed the

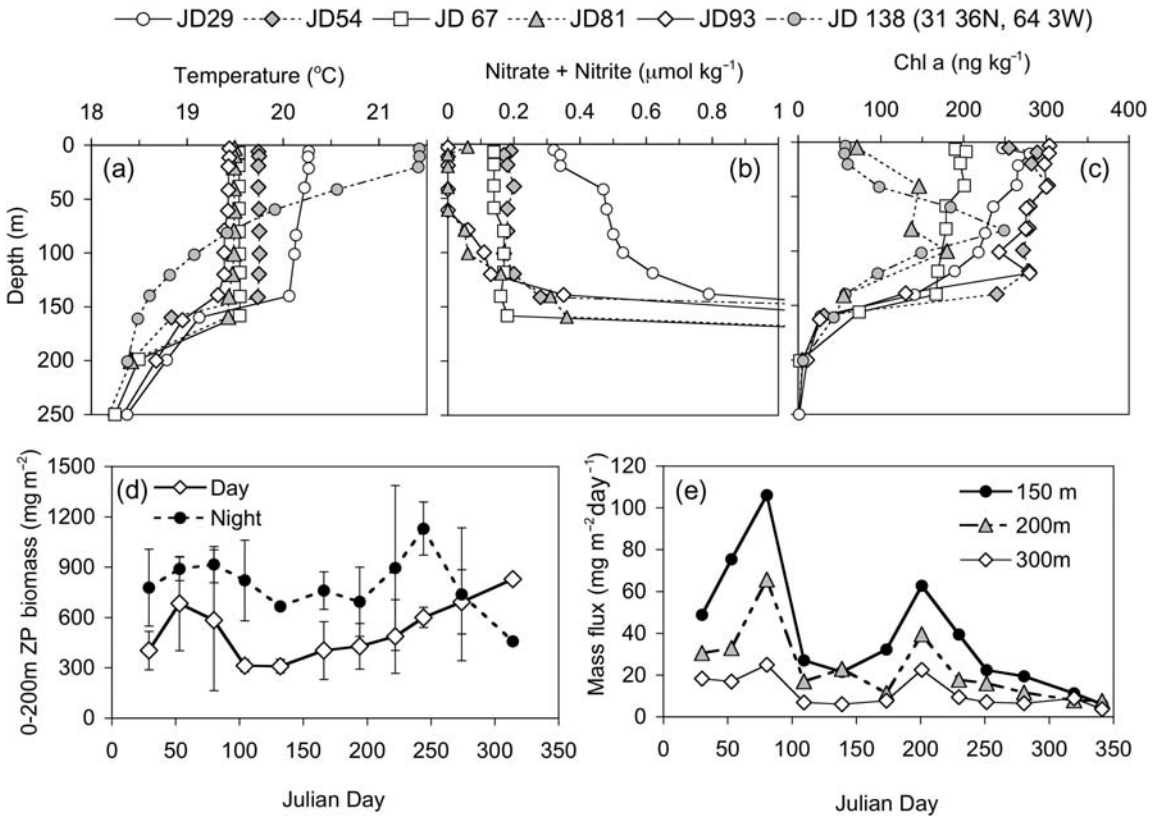

Fig. 3. Physical and biological properties of the upper ocean at the BATS site. (**a**) Temperature profiles (**b**) Nitrite and nitrate concentration profiles (**c**) Chlorophyll a concentration profiles (**d**) Integrated 0–200 m mesozooplankton dry weight in day and night tows, using a meter square 202 μm mesh net (Steinberg *et al.*, 2001). (**e**) The mass flux at depths of 150, 200 and 300 m from drifting (PITS) sediment traps.

previous months at the BATS site and exceeded the nighttime zooplankton biomass observed in Eddy C in March (Fig 3d). Additionally, the ADCP backscatter intensity, measured on the nearby BTM mooring, also increased significantly as Eddy A passed over the site and indicated that the mesozooplankton biomass in the frontal boundary of Eddy A was strongly elevated over that in surrounding waters (Smeti *et al.*, 2010).

Three-day drifting trap fluxes at depths of 150, 200 and 300 m depth (mg dry weight $m^{-2}\,day^{-1}$) were correlated with changes in the phytoplankton and zooplankton biomass (Fig. 3e). Fluxes increased as Eddy C passed through (JD 53 and 80), especially at depths of 150 and 200 m, but decreased by 25% as Eddy C moved away (JD 109). Drifting trap fluxes remained low as Eddy M passed over. Drifting trap fluxes increased in July but this increase did not appear to be related to any mesoscale feature. Interestingly, no increase was observed in drifting trap fluxes as Eddy A passed through despite the elevated zooplankton biomass in the frontal boundary of Eddy A. This suggested that any increase in particle production was efficiently recycled within the surface waters.

Temporal variability in mass, organic carbon and aggregate fluxes at a depth of 1500 m

As Eddy C passed over in late February–early March, the total mass flux, POC flux and aggregate flux all rose sharply, with the mass flux increasing by a factor of four (Fig. 4a). The maximum in the mass flux (130 mg dry weight $m^{-2}\,day^{-1}$) and the POC flux (8 mg $m^{-2}\,day^{-1}$) was more than twice that typical of the spring peak at this depth (Conte *et al.*, 2001). The flux of amorphous aggregates, as well as of several microzooplankton species was exceptional (Fang *et al.*, 2010), and clearly indicated that the bloom conditions within Eddy C had a major effect on the export flux.

As Eddy C moved away and Eddy M began to influence the site, the mass flux declined and remained low for the remainder of the year. The minimal influence of Eddy M on the deep particle flux is consistent with the low surface export flux from Eddy M in its post-bloom status (Fig. 3e). Even so, Eddy M did have a small influence on the aggregate flux, which increased slightly as Eddy M passed through. The aggregate flux also increased briefly in July (JD 190–220), during the same time period when the zooplankton biomass and the drifting trap fluxes increased at the BATS site (Fig. 3d and e).

The mass flux at a depth of 1500 m did not increase as Eddy A passed through the site despite the elevated zooplankton biomass (Fig. 3d, Smeti *et al.*, 2010) observed in the periphery of Eddy A (Fig. 4a). This lack of any increase in the deep flux was consistent with the drifting trap data (Fig. 3e), and indicated that there was no substantial enhancement of the surface export flux associated with Eddy A.

Temporal variability of fecal pellet flux at a depth of 1500 m

Seasonality in the fecal pellet flux at a depth of 1500 m was small in comparison with the variability associated with the passage of the eddy (Fig. 4). The numerical flux of fecal pellets was generally correlated with that of the total mass and carbon flux (Fig. 4a). The fecal pellet flux averaged 198 ± 75 pellets $m^{-2}\,day^{-1}$ and varied by a factor of five, from a maximum of 420 pellets $m^{-2}\,day^{-1}$ when Eddy C passed over the site (mid-date JD 42) to a minimum of 90 pellets $m^{-2}\,day^{-1}$ just after the passage of Eddy C (mid-date JD 96) (Fig. 4b). In contrast, only a small increase in the fecal pellet flux was observed as Eddy M passed through (JD 110-140). The numerical pellet flux also increased slightly when Eddy A passed through (JD 263-308), but this was not temporally coincident with the eddy and may not have been related to the eddy conditions.

The fecal pellet size varied with the passage of the eddy (Fig. 4b). The mean fecal pellet size averaged $5.4 \pm 0.9 \times 10^{-3}\,mm^3$ and ranged from $3.8 \times 10^{-3}\,mm^3$ to $7.7 \times 10^{-3}\,mm^3$. The median pellet size was less variable and smaller ($3.0 \times 10^{-3}\,mm^3$), indicative of strongly skewed pellet size distributions (see below). The mean pellet size decreased from $5.5 \times 10^{-3}\,mm^3$ to $3.7 \times 10^{-3}\,mm^3$ as Eddy C passed through. This decrease suggested that smaller sized individuals comprised the zooplankton community, as the pellet size correlates with the body size (Uye and Kaname, 1994). Conversely, the mean fecal pellet size increased from $4.9 \times 10^{-3}\,mm^3$ to $5.9 \times 10^{-3}\,mm^3$ as Eddy M passed through, which suggested larger individuals in the zooplankton community. The mean fecal pellet size increased by roughly 60% as Eddy A passed through (mid-dates JD 232 to JD 249), also suggesting larger zooplankton individuals within the frontal boundary of Eddy A.

The fecal pellet fluxes and their contribution to the total carbon flux were more variable than the total mass and POC fluxes (Fig. 4c). The fecal pellet mass flux (dry weight) averaged 1.14 mg $m^{-2}\,day^{-1}$ and varied by nearly a factor of four, from 0.5 mg $m^{-2}\,day^{-1}$ to 1.9 mg $m^{-2}\,day^{-1}$. Assuming an average carbon content of 0.08 mg C mm^{-3}, this equated to an average

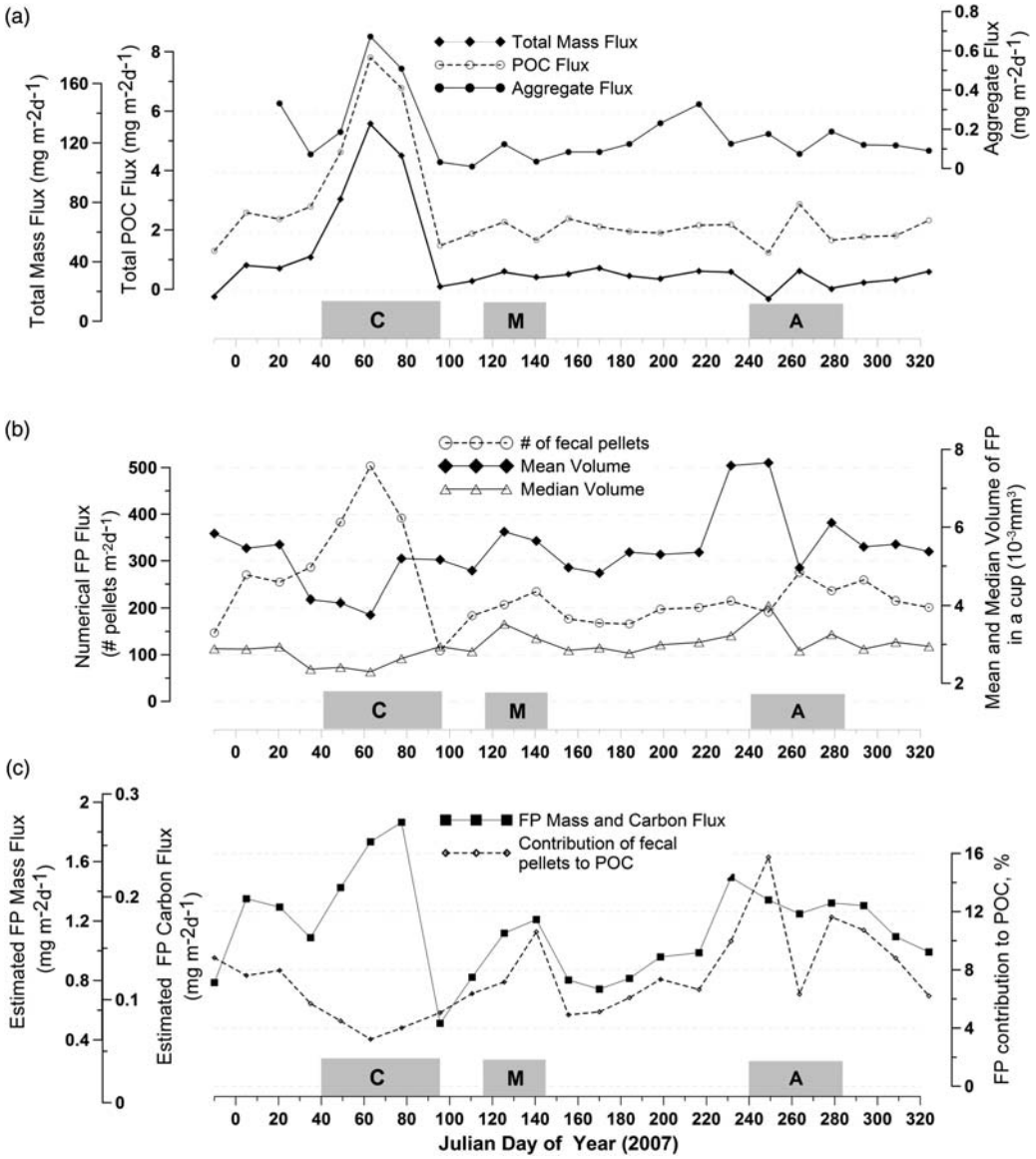

Fig. 4. (**a**) Temporal variation in the total mass flux, particulate organic carbon flux and aggregate flux at a depth of 1500 m. The mid-date of each sampling period is plotted. The gray bars indicate approximate time periods when the cyclonic (C), mode water (M) and anticyclonic (A) eddies were over the OFP site. The eddy periphery is operationally defined as an SLA contrast of 5 cm. (**b**) Temporal variability in the fecal pellet number, and in the mean and median pellet volumes. (**c**) Temporal variation in the fecal pellet mass and carbon fluxes (mg m^{-2} day^{-1}), and in the fecal pellet percentage of the total organic carbon flux.

carbon flux of 0.17 mg m^{-2} day^{-1} (range of 0.07–0.27 mg C mg m^{-2} day^{-1}), or between 3 and 16% of the total organic carbon flux at a depth of 1500 m.

The fecal pellet fluxes and contribution to the total carbon flux varied with the passage of the eddy (Fig. 4c). As Eddy C passed through the site, a large increase in the fecal pellet mass flux was observed, with the fecal pellet flux reaching its maximum value for the entire time period. Even so, fecal pellets comprised only 3% of the total organic carbon flux, the minimum value over the entire time period, due to the extreme flux of amorphous aggregates in Eddy C. As Eddy M passed through, the fecal pellet flux also increased, though less dramatically, from 0.8 to 1.2 mg m^{-2} day^{-1}, whereas the fecal pellet contribution to the total carbon flux doubled. Following the passage of Eddy M, the fecal pellet mass flux declined to 0.8 mg m^{-2} day^{-1}, or 5% of the total carbon flux. As Eddy A arrived, the fecal pellet mass and carbon flux increased by nearly 50% due to the increased fecal pellet size. The fecal pellet mass flux over the remainder of the autumn period remained high (1.0–1.4 mg m^{-2} day^{-1})

and comprised 6–8% of the total organic carbon flux.

Change in the fecal pellet flux with depth

The 500 and 3200 m traps were analyzed during the 2-month time period when Eddies C and M passed through to assess the change in the fecal pellet flux with depth (Fig 5). Over this period, we did not observe any major difference in fecal pellet morphology or in pellet color.

The fecal pellet numerical flux and mass flux at a depth of 500 m was only ~50% that measured at a depth of 1500 m. Numerical fluxes averaged 103 pellets m^{-2} day^{-1} at a depth of 500 m (49–177 range), 223 pellets m^{-2} day^{-1} at 1500 m depth (108–392 range) and 192 pellets m^{-2} day^{-1} at a depth of 3200 m (119–291 range). Fecal pellet mass fluxes averaged 0.46 mg m^{-2} day^{-1} (range 0.27–0.86 mg m^{-2} day^{-1}) at a depth of 500 m and increased to 1.08 mg m^{-2} day^{-1} (range 0.51–1.86 mg m^{-2} day^{-1}) at a depth of 1500 m. The fecal pellet mass flux at a depth of 3200 m was less variable and averaged 0.61 mg m^{-2} day^{-1} (range 0.42–0.83 mg m^{-2} day^{-1}), ~40% of that at a depth of 1500 m.

The fecal pellet contribution to the total mass flux decreased with depth, averaging 3.2% (0.3–5.4% range) at 500 m depth, 2.6% (1.7–3.3% range) at a depth of 1500 m and 1.5% (0.6–2.4% range) at 3200 m depth (Fig. 5b). This decrease primarily reflected the decrease in the organic carbon content of the flux. When normalized to organic carbon, there were no depth-related trends in the fecal pellet contribution, which averaged

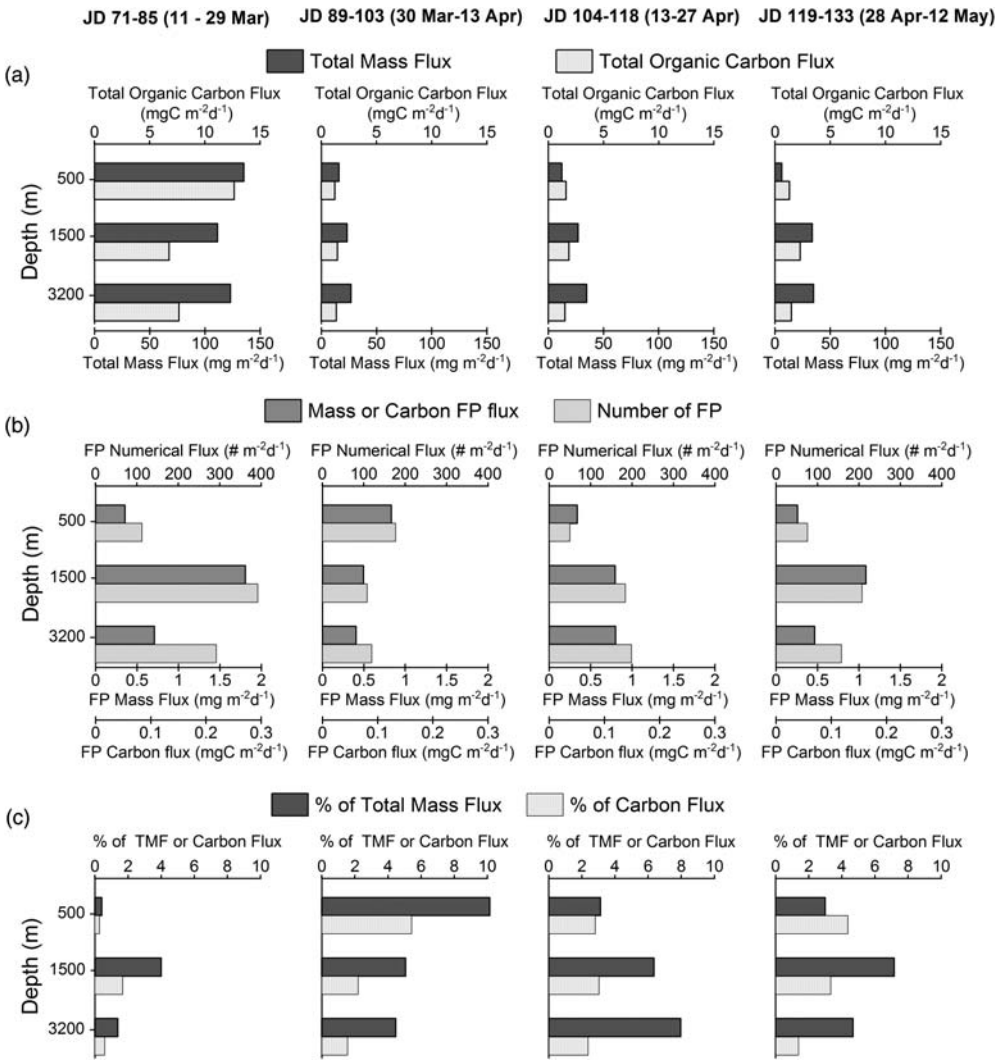

Fig. 5. Depth changes in (**a**) total mass and total organic carbon fluxes, (**b**) fecal pellet (FP) numerical flux and mass and carbon fluxes and (**c**) the fecal pellet contribution to total mass and organic carbon fluxes. The time period analyzed covers the period when the cyclonic (C) and mode water (M) eddies passed over the site (c.f. Fig 3).

4.2, 5.6 and 4.6% of the carbon flux at depths of 500, 1500 and 3200 m, respectively.

Little temporal correlation was observed in the fecal pellet flux, pellet size or fecal pellet contribution of the total mass or organic carbon flux among the three trap depths. For example, in the sample collection period between JD 89–103, there was a maximum in the fecal pellet mass flux at a depth of 500 m but a minimum at 1500 and 3200 m. The only correspondence among the different depths was observed during the passage of Eddy C (JD 71-85), when the pellet contribution to the mass and organic carbon fluxes was at a minimum at all depths due to dilution by the high aggregate flux (Fig. 4a and b).

Fecal pellet size frequency distributions

Fecal pellet size frequency distributions were strongly skewed in all samples (Fig. 6). As for other environmental variables, pellet size distributions were gamma distributed. To quantitatively assess changes in distributions over time and with depth, we fitted the empirical size frequency distributions to model gamma distributions (EasyFit, Mathwave Technologies). A four-parameter gamma probability model best approximated the empirical distributions:

$$f(x) = \frac{k(x-y)^{k\alpha-1}}{\beta^{k\alpha}\gamma(\alpha)}\exp(-((x-y)/\beta)^{k})$$

where k and α are continuous, non-negative shape parameters, and β and γ are continuous, non-negative scale parameters. As shown in Fig. 6, the modeled distributions closely fitted the sample distributions although slightly underestimated the distribution peak. The skewness of the fecal pellet size distributions was uncorrelated with either the mean or median fecal pellet size (Fig. 7).

Figure 8 compares the temporal variability in the skewness of the fecal pellet size distributions at a depth of 1500 m with the mean and median pellet sizes. Prior to the passage of Eddy C, the skewness and mean and median fecal pellet sizes were higher than the average but decreased sharply as Eddy C passed through the site. This decrease was associated with an increase in the abundance of small spherical pellets indicative of production by immature zooplankton stages. As Eddy C moved away (JD 70-88), the mean pellet size and the skewness both increased briefly but, as Eddy M began to influence the site, skewness sharply declined to minimum values. Between JD 160 and 230 skewness was variable and the pellet size remained relatively stable. As Eddy A passed by in late August (mid-date JD 255), the fecal pellet size increased by 25% but there was minimal change in sample skewness. As Eddy A moved away, skewness increased to near maximum values, whereas the pellet size decreased. Pellet sizes and sample skewness remained above average throughout the remainder of the autumn period.

There were no consistent differences in the fecal pellet size or size distributions with depth over the short time interval we studied, although the variability among samples was lower at a depth of 3200 m than at a depth of 500 m (Fig. 9). The mean pellet size was similar at 500 and 1500 m depths, averaging 4.4×10^{-3} mm^3

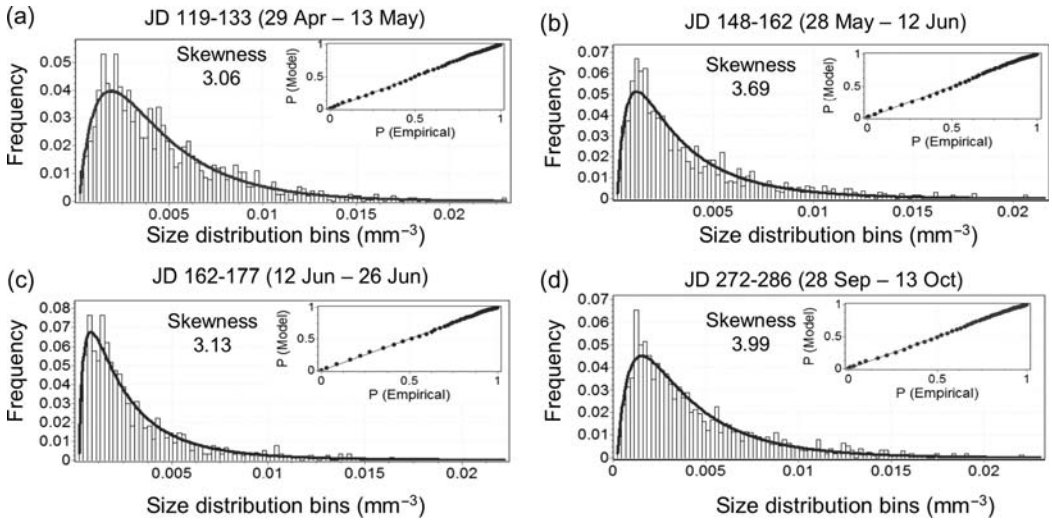

Fig. 6. Representative samples showing the range in the empirical and modeled fecal pellet size frequency distributions at a depth of 1500 m. The heavy black line overlying the sample distributions shows the modeled gamma distribution (see text). The model goodness of fit is shown by the plots of empirical vs. model cumulative probabilities in the top right corner of each graph. The skewness parameter of each model distribution is shown within the graph.

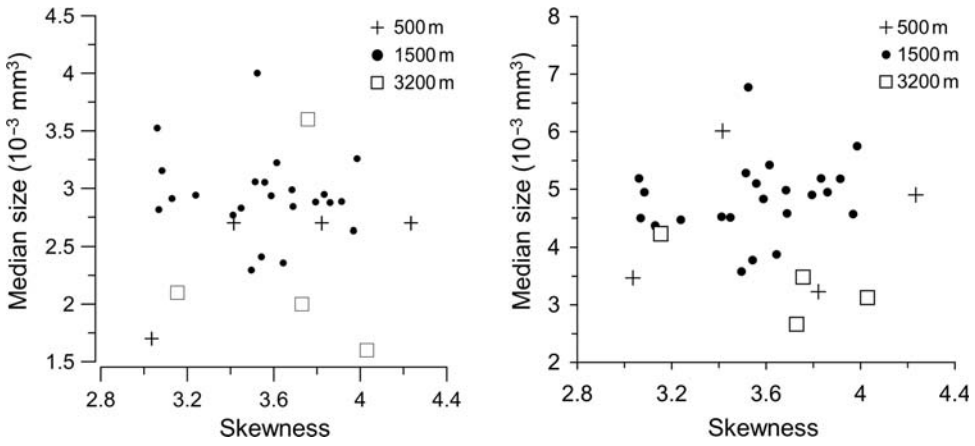

Fig. 7. Relationship between the (**a**) median and (**b**) mean fecal pellet size and skewness parameter of the model size distributions.

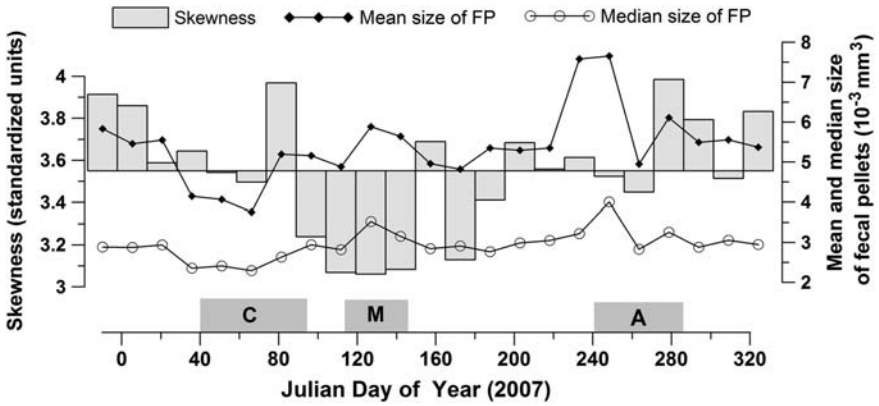

Fig. 8. Temporal variability in mean and median fecal pellet sizes and the skewness parameter of the size distributions at a depth of 1500 m. The mean fecal pellet size and the skewness parameter are plotted relative to their mean value over the time series. The gray bars indicate the approximate periods when the cyclonic (C), mode water (M) and anticyclonic (A) eddies were over the OFP site.

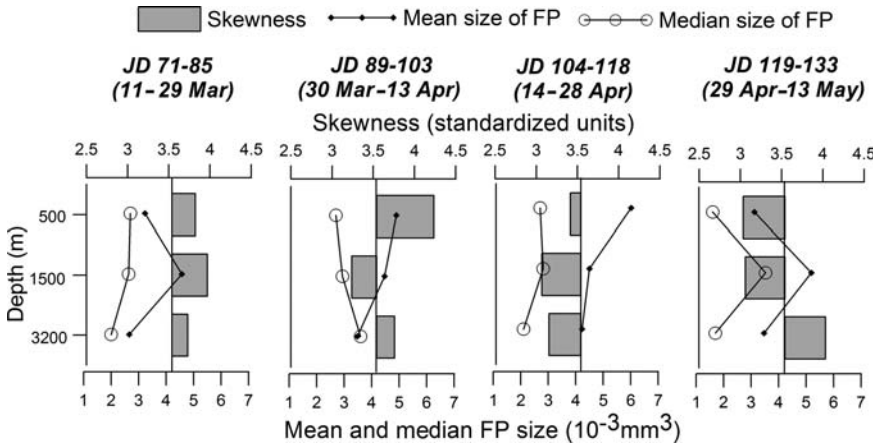

Fig. 9. Depth changes in the mean and median fecal pellet sizes and the skewness parameter of the sample size distributions. The mean fecal pellet size and the skewness parameter are plotted relative to their mean values, averaged for all depths over the period of observation (i.e. JD 71–JD 133).

and 4.7×10^{-3} mm^3, respectively. At a depth of 3200 m, the mean pellet size (3.4×10^{-3} mm^3) was ~25% smaller and also less variable, ranging from 3.1×10^{-3} mm^3 (JD 119-133) to 4.2×10^{-3} mm^3 (JD104-118). The Sample skewness was variable at each depth with no apparent depth trend.

Differences in both pellet size and pellet size distributions point to distinct fecal pellet populations at the three sampling depths, as well as marked temporal variability (Fig. 9). For example, during the 30 March–13 April (JD 89-03) sampling period, the mean pellet size decreased uniformly with depth, whereas the skewness of the pellet size distribution decreased strongly between depths of 500 and 1500 m and then increased again at a depth of 3200 m. During the 14-28 April (JD 104–118) period, the mean pellet size and sample skewness at depths of 1500 and 3200 m were similar. Conversely, during the 29 April–13 May (JD 119-133) period, the sample skewness was similar at depths of 500 and 1500 m depths but the pellet size at a depth of 1500 m was 50% greater than at a depth of 500 m. During the same period the fecal pellet size at a depth of 3200 was similar to that at 500 m, but the pellet size distribution was more highly skewed.

DISCUSSION

Seasonal and mesoscale eddy influences on the fecal pellet flux variability

Seasonality in the fecal pellet flux at the OFP site was small in comparison with the influence of mesoscale eddies (although the typical influence of the spring bloom was confounded by the presence of Eddy C). The enhancement in the fecal pellet flux, and in particular the sharp increase in the flux of small ovoid pellets as Eddy C passed through mirrors the *in situ* upper ocean data indicating that zooplankton production was strongly stimulated by the developing bloom in Eddy C. Stimulation of zooplankton production has been previously observed in the surface waters of productive eddies in the Sargasso Sea (Goldthwait and Steinberg 2008; Eden *et al.*, 2009), off the Hawaiian islands (Landry *et al.*, 2008), in the northeast Atlantic (Labat *et al.*, 2009) and off the west coast of Australia (Strzelecki *et al.*, 2007). Yebra *et al.* (Yebra *et al.*, 2005) also observed higher primary production, and a higher zooplankton biomass and respiratory fluxes down to 900 m in an anticyclonic eddy off the Canary islands, and suggested that the eddy conditions enhanced vertical migration from the deep scattering layer which, in turn, increased the zooplankton active flux, However, none of these studies has definitively linked the passage of productive eddies with changes in the mesopelagic fecal pellet flux. Our data conclusively show that the biological consequences of mesoscale physical variability in the surface ocean can be very efficiently transferred via sinking fecal pellets to mesopelagic depths.

In contrast to Eddy C, the influence of Eddy M on the mesopelagic mass or carbon flux was minimal as it passed over the site, despite the fact that Eddy M was at least as productive as Eddy C, only a few weeks earlier (Krause *et al.*, 2010). The comparison underscores the transience of eddy-driven enhancement of the export flux, with important implications for modeling eddy influences on export fluxes based solely upon remote sensing.

The mean size of the fecal pellet flux increased when Eddy M and especially Eddy A passed through the site. As the pellet size is strongly correlated with the zooplankton body size (Uye and Kaname, 1994), this increase suggests that the zooplankton communities that had developed in these eddies were composed of larger individuals than in the surrounding waters. Deevey (Deevey, 1964) observed that in the Sargasso Sea copepods, size correlated with phytoplankton concentration rather than temperature. Our data are consistent with this observation. If the zooplankton size is controlled primarily by food availability in the Sargasso Sea, then mesoscale eddies, by influencing non-seasonal productivity patterns, may also alter the mean size of zooplankton. This, in turn, could have an influence on the carbon penetration depths, as larger zooplankton produce larger, more rapidly settling fecal pellets that would more efficiently transfer material through the water column (e.g. Lampitt, 1990; Wassmann, 1998).

Fecal pellet contribution to carbon flux

Intact zooplankton fecal pellets were a minor contribution to the total organic carbon flux at all depths. Using a carbon conversion factor of 0.08 mgC mm^{-3}, fecal pellets contributed on average 4.2% (range 0.4–10.0%) of the carbon flux at a depth of 500 m, 7.5% (range 3–16%) of the carbon flux at a depth of 1500 m and 4.6% (range 1.4–8.0%) of the carbon flux at a depth of 3200 m. These estimates are similar to results of several other studies of the fecal pellet flux in mesopelagic and bathypelagic waters (*Table I*). However, some studies have estimated much higher fecal pellet contributions to the deep water carbon flux. For example, in the upwelling region off Chile, fecal pellets were estimated to contribute 17% of the carbon flux at a depth of 2300 m in spring and up to 44% in other seasons (Gonzalez *et al.*, 2004). In the Mediterranean, Carroll *et al.* (Carroll *et al.*, 1998) estimated that fecal pellets contributed on average

Table I: Literature values of the fecal pellet carbon (FPC) flux and the fecal pellet percentage of the total organic carbon flux (TCF) in the mesopelagic and bathypelagic waters of different ocean regions

Region	Depth (m)	FPC flux (mg C m^{-2} day^{-1})	% of TCF[a]	Reference
Mesopelagic and bathypelagic waters				
Sargasso Sea	500	0.07–0.12	4.2 (0.4–10.0)	This study
Sargasso Sea	1500	0.07–0.27	7.4 (3.2–15.7)	This study
Sargasso Sea	3200	0.03–0.12	4.6 (1.4–8.0)	This study
Mediterranean Sea (DYFAMED)	500	0.2–3.2	14[b]	(Carroll *et al.*, 1998)
Mediterranean Sea (DYFAMED)	1000	0.1–5.8	23[b]	(Carroll *et al.*, 1998)
Mediterranean Sea (DYFAMED)	2000	—	8[b]	(Carroll *et al.*, 1998)
Mediterranean Sea	1500	0.30	5.3	(Wassmann *et al.*, 2000)
Central N Pacific	4280	0.01	1.1	(Pilskaln and Honjo, 1987)
Central N Pacific	5582	0.01	1.4	(Pilskaln and Honjo, 1987)
Central N Pacific (ALOHA)	500	1.5	35 ± 23	(Wilson *et al.*, 2008)
NW Pacific (K2 deployments 1 and 2)	500	0.8, 0.7 ± 0.6	2.8, 5.6 ± 4.8	(Wilson *et al.*, 2008)
NE Pacific	500	0.06	9.5	(Urrère and Knauer, 1981)
NE Pacific	750	0.04	6.6	(Urrère and Knauer, 1981)
NE Pacific	1500	0.06	3.4	(Urrère and Knauer, 1981)
Chilean coast	2300	<1.0–5.0	35.4 (3–99)[c]	(Gonzalez *et al.*, 2004)
Tropical Atlantic	988	0.26	6.7	(Pilskaln and Honjo, 1987)
Tropical Atlantic	3755	0.14	8.3	(Pilskaln and Honjo, 1987)
Tropical Atlantic	5068	0.16	9.3	(Pilskaln and Honjo, 1987)
Panama Basin	667	1.02	8.1	(Pilskaln and Honjo, 1987)
Panama Basin	1268	0.09	1.1	(Pilskaln and Honjo, 1987)
Panama Basin	2869	0.11	1.0	(Pilskaln and Honjo, 1987)
Panama Basin	3769	1.50	13.2	(Pilskaln and Honjo, 1987)
Panama Basin	3791	1.40	13.8	(Pilskaln and Honjo, 1987)
Norwegian Sea	950–1000	0.5–6	<10	(Bathmann *et al.*, 1987)
Upper mesopelagic waters (150–300 m)				
Sargasso Sea (inside, outside eddies)	150	0.8–1.7, 0.6–1.9	5–12, 4–7	(Goldthwait and Steinberg, 2008)
Mediterranean Sea (DYFAMED)	200	1.0–7.0	24[b]	(Carroll *et al.*, 1998)
Mediterranean Sea	200	0.1–19.4	23 (2–62)	(Miquel *et al.*, 1994)
Mediterranean Sea	200	0.18	5.8	(Wassmann *et al.*, 2000)
Northeast subtropical Atlantic	200	1–49	42 (10–80)	(Huskin *et al.*, 2004)
Tropical Atlantic	389	0.23	3.4	(Pilskaln and Honjo, 1987)
Central N Pacific (ALOHA)	150	2.1	14.2 ± 9.6	(Wilson *et al.*, 2008)
Central N Pacific (ALOHA)	300	1.5	22.1 ± 23.1	(Wilson *et al.*, 2008)
NE Pacific, California current	150	0.36	19.0	(Urrère and Knauer, 1981)
North Pacific central Gyre	200	0.05–0.50	0.2–1.2	(Taylor, 1989)
NW Pacific (K2 deployments 1 and 2)	150	7.6 ± 0.4, 6.7 ± 1.4	12.1 ± 0.6, 28.5 ± 3.6	(Wilson *et al.*, 2008)
NW Pacific (K2 deployments 1 and 2)	300	6.9 ± 0.8, 3.2 ± 0.0	14.7 ± 0.5, 20.0 ± 3.0	(Wilson *et al.*, 2008)
Chilean upwelling (preEl Nino, El Nino)	200	3.7–8.2, 5.1–61.7	5.2–13.0, 13.3–94.3	(Gonzalez *et al.*, 2000)
Chilean upwelling (preEl Nino, El Nino)	300	1.1–9.1, 7.2–16.4	5.4–7.6, 17.5–89.2	(Gonzalez *et al.*, 2000)
Barents Sea	200	<5–220	20 ± 7	(Wexels Riser *et al.*, 2008)
Norwegian Sea	250–300	3–17	<10	(Bathmann *et al.*, 1987)
Ross Sea	200	0.2–2.4[b]	6.0–21.1[c]	(Smith *et al.*, 2011)
Ross Sea	200	4.6–54.5	5–48	(Gowing *et al.*, 2001)

[a]Average (range).
[b]Annual averages.
[c]December–March yearly averages.

8% of the carbon flux at a depth of 2000 m, only slightly higher than our estimates. However, fecal pellets were estimated to contribute 14 and 23% of the carbon flux at depths of 500 and 1000 m, respectively. Also unlike our study, the fecal pellet fraction of the carbon flux in the Mediterranean varied seasonally, from 20–35% in winter–spring to <5% in late summer–autumn (Carroll *et al.*, 1998). In the Northwest Pacific off Japan, similarly high and variable percentages of the fecal pellet contribution to the total carbon flux have been observed (Wilson *et al.*, 2008).

In the upper mesopelagic zone, the fecal pellet fraction of the total carbon flux tends to be higher and also more variable (*Table I*). The fecal pellet fraction of the total carbon flux in several oligotrophic regions appears to be similar to or only slightly higher than our estimates. For example, fecal pellets contributed on average 5–12% of the carbon flux at a depth of 150 m in the Sargasso Sea (Goldthwait and Steinberg, 2008), 6% of the carbon flux at a depth of 200 m in the Mediterranean Sea (Wassmann *et al.*, 2000), 3% of the carbon flux at a depth of 400 m in the western tropical

Atlantic (Pilskaln and Honjo, 1987) and 1% of the carbon flux at a depth of 200 m in the North Pacific gyre (Taylor, 1989) . However, other studies have estimated much higher and more variable fecal pellet flux and contribution to the total carbon flux. In the northeastern subtropical Atlantic, Huskin *et al.* (Huskin *et al.*, 2004) estimated that fecal pellets contributed from 10 to 80% of the carbon flux at a depth of 200 m. In the Chilean upwelling region, Gonzalez *et al.* (Gonzalez *et al.*, 2004) estimated that fecal pellets contributed between 5 and 13% of the flux in the upper 300 m in non-ENSO years, but that the fecal pellet contribution increased to 13–94% of the total carbon flux in ENSO years. Similarly Wilson *et al.* (Wilson *et al.*, 2008) also observed a two-fold increase in the fecal pellet fraction of the carbon flux at the K2 site in the northwestern Pacific, which was associated with differences in productivity at the time of sampling. Extreme temporal and interannual variability in the fecal pellet fraction of the organic carbon flux at a depth of 200 m has also been observed in the Ross Sea, where the fecal pellets comprise <10% of the carbon flux in some years and >20% of the carbon flux in other years, and nearly 100% of the flux for short intervals (Smith *et al.*, 2011). Overall, these studies suggest that, as productivity increases, fecal pellets contribute more to the carbon flux, reflecting a positive correlation between primary production, zooplankton biomass and pellet production rates.

Estimates of fecal pellet contribution to the carbon flux in these studies are only approximate as the carbon content of fecal pellets is poorly constrained. For surface-dwelling copepods, the carbon content of fecal pellets may vary by as much as 50% depending upon the taxa and feeding environment (Urban-Rich *et al.*, 1998). Less is known about fecal pellets produced by mesopelagic and bathypelagic species. If their carbon content also varies with food supply, then the actual contribution of fecal pellets to the carbon flux at depth may be much more variable and underestimated during periods, such as the passage of productive eddies, when large pulses of labile bioavailable material are encountered. Clearly, more studies are needed to better constrain the carbon content of fecal pellets of mesopelagic zooplankton communities and elucidate how pellet production and composition may be affected by the feeding environment.

Despite this uncertainty, our data clearly indicate that intact fecal pellets are a relatively minor component of the deep carbon flux in the Sargasso Sea. This conclusion is not surprising as most of the mass and organic carbon in OFP trap samples is found in smaller size fractions and in largely disintegrated form (Deuser *et al.*, 1981; Conte *et al.*, 2001; personal observations). The high percentages of fragmented pellets observed in deep sediment traps (e.g. Wilson *et al.*, 2008) suggest that a potentially large fraction of pellet production is rendered unrecognizable by coprohexy in the water column. In the OFP sediment traps, scanning electron microscopy reveals abundant broken frustules, tests and other remains of the fecal pellets in the <125 μm fraction (unpublished data). Although the fecal contribution to the carbon in this fraction is not quantifiable using microscopic techniques, the analysis of diagnostic fecal biomarkers could aid in providing a first-order estimate.

Depth variability of fecal pellet flux

No consistent trends with depth were observed in the fecal pellet number, flux or size distributions over the limited time period we examined. Previous studies similarly have observed marked shifts in the fecal pellet flux and in its morphology and composition with depth (e.g. Bishop *et al.*, 1980; Urrère and Knauer, 1981; Fowler and Knauer, 1986; Bathmann *et al.*, 1987; Lampitt *et al.*, 1990; Carroll *et al.*, 1998; Wilson *et al*, 2008). Overall, these studies provide evidence for intense recycling of the fecal pellet flux within the water column and indicate that the pellet assemblage more closely reflects the resident zooplankton community at that depth rather than production by zooplankton populations in overlying waters.

Although some of the depth variability that we observed could reflect lateral variability arising from the different collection "cones" of deep sediment traps (e.g. Siegel and Armstrong, 2002), our data are consistent with the interpretation that pellet assemblages reflect a dynamic balance between the flux from the overlying water column, zooplankton consumption and flux recycling processes and *in situ* production of fresh pellets at the sampling depth. For example, as Eddy C passed over the site (Fig. 9, JD 119-133), the mean fecal pellet size at a depth of 500 m was at a minimum. However, the mean pellet size at a depth of 1500 m was 50% larger than at a depth of 500 m, and the pellet flux was four times higher. Thus, most pellets sampled at a depth of 1500 m could not have been sourced directly from overlying waters but likely were produced *in situ* by a larger sized zooplankton community feeding on the surface export flux.

A particularly interesting observation is the lack of any consistent decrease in the fecal pellet size with depth over the interval we studied. As particle settling rates tend to increase with depth (Berelson, 2001), an increase in the pellet size with depth might be expected. The observation that the pellet size does not increase

suggests that the increase in settling rates may be due to an increase in pellet density rather than the pellet size. Additionally, larger particles sink more rapidly and have shorter exposure to recycling processes within the water column, which should positively skew the size distribution of the pellet flux relative to that in overlying waters. Alternatively, if fecal pellets are rapidly recycled via coprophagy, size distributions will more strongly reflect pellet production at that depth, as edited by differential grazing pressure, rather than particle size sorting. If this is the case, then the rather consistent pellet size at the three trap depths suggests that the mean size of the zooplankton communities at these depths is similar. This interpretation is consistent with the relatively small size differences observed in zooplankton tows at depths of 500 and 2000 m in the Sargasso Sea (Deevey and Brooks, 1977). Alternatively, the mean pellet size in deeper water may be larger but grazing pressure is more intense on larger sized particles and edits the pellet size distributions. The relative importance of these processes in controlling pellet size distributions in deep waters remains to be explored.

Summary and conclusions

In the mesopelagic Sargasso Sea, seasonal trends in the fecal pellet flux and the size distribution are small in comparison with variability arising from the influence of mesoscale eddies on zooplankton production and fecal pellet generation. The large shifts in the fecal pellet flux and the size distribution during the passage of an eddy underscore the efficiency with which transient changes in overlying surface waters propagate to mesopelagic depths, and furthermore suggest that the mesopelagic zooplankton community experiences the effects of upper ocean mesoscale variability. The absence of consistent correlations or depth trends in the numerical flux or fecal pellet size distributions provides additional evidence for intense particle recycling within the deep water column.

Intact fecal pellets contribute only a minor fraction (3–16%) of the total carbon flux in the deep Sargasso Sea. Although the fecal pellet contribution to the mass and carbon flux is quantitatively minor, detailed analyses of fecal pellets can provide significant insights on deep-dwelling zooplankton and midwater ecosystem processes that influence the deep particle flux. Additional studies linking the fecal pellet flux to seasonal and non-seasonal forcing, along with a better understanding of the processes controlling mesopelagic zooplankton grazing and fecal pellet production, will greatly enhance our understanding of the role of midwater zooplankton on particle flux recycling. Quantitative image analysis can significantly facilitate this effort and the promise of this approach continues to expand with ongoing improvements in digital image acquisition and analysis.

ACKNOWLEDGEMENTS

This research was initiated as part of the Nippon Foundation—Partnership for Observations of the Global Oceans (POGO) Centre of Excellence hosted at the Bermuda Institute of Ocean Sciences, where Olga Shatova was a scholar during 2009–2010. We thank the captain and crew of the R/V Atlantic Explorer for their able assistance with OFP mooring turnarounds and J.C. Weber, Jean Fang and Rachel Franzblau for their assistance with OFP sample processing. The faculty, staff and students at BIOS are thanked for helpful comments during this research. We thank Tommy Dickey for access to unpublished data and the many BATS technicians and principal investigators for their contribution to the BATS data resources. We thank the NSF Chemical Oceanography Program for the continuous support of the Oceanic Flux Program time-series over more than 30 years, most recently by grants OCE 092285 and OCE 0623505. We also thank the Nippon Foundation and POGO for their support of the Nippon-POGO Centre of Excellence at BIOS.

REFERENCES

Alldredge, A. (2001) Particle aggregation dynamics. In Steele, J. H. (ed), *Encyclopedia of Ocean Sciences 2001*, Elsevier Science Ltd., Oxford, pp. 2090–2097.

Angel,, M. V. (1989) Does mesopelagic biology affect the vertical flux? In Berger, W. H., Smetacek, V. S. and Wefer, G. (eds), *Productivity of Oceans, Past and Present*, John Wiley & Sons, New York, pp. 155–173.

Atkinson, A., Schmidt, K., Fielding, S. *et al.* (2012) Variable food absorption by Antarctic krill: relationships between diet, egestion rate and the composition and sinking rates of their fecal pellets. *Deep Sea Res. I.*, **59–60**, 147–158.

Bathmann, U. V., Noji, T. T., Voss, M. *et al.* (1987) Copepod fecal pellets: abundance, sedimentation and content at a permanent station in the Norwegian Sea in May/June 1986. *Mar. Ecol. Prog. Ser.*, **38**, 45–51.

Berelson, W. M. (2001) Particle settling rates increase with depth in the ocean. *Deep-Sea Res. II*, **49**, 237–251.

Bishop, J. K. B., Collier, R. W., Ketten, D. R. *et al.* (1980) The chemistry, biology and vertical flux of particulate matter from the upper 1500 m of the Panama basin. *Deep-Sea Res.*, **27**, 615–640.

Carroll, M. L., Miquel, J. C. and Fowler, S. W. (1998) Seasonal patterns and depth-specific trends of zooplankton fecal pellet fluxes in the Northwestern Mediterranean Sea. *Deep-Sea Res. I*, **45**, 1303–1318.

Conte, M. H., Dickey, T. D., Weber, J. C. *et al.* (2003) Transient physical forcing of pulsed export of bioreactive material to the deep Sargasso Sea. *Deep-Sea Res. I*, **50**, 1157–1187.

Conte, M. H., Ralph, N. and Ross, E. (2001) Seasonal and interannual variability in deep ocean particle fluxes at the Oceanic Flux Program/Bermuda Atlantic Time-series (BATS) site in the western Sargasso Sea near Bermuda. *Deep-Sea Res. II*, **48**, 1471–1505.

Conte, M. H., Weber, J. C. and Ralph, N. (1998) Episodic particle flux in the deep Sargasso Sea: an organic geochemical assessment. *Deep-Sea Res. I*, **45**, 1819–1841.

Deevey, G. B. (1964) Annual variations in length of copepods in the Sargasso Sea off Bermuda. *J. Mar. Biol. Assoc. U. K.*, **44**, 589–600.

Deevey, G. B. and Brooks, A. L. (1977) Copepods of the Sargasso Sea off Bermuda: species composition, and vertical and seasonal distribution between the surface and 2000 m. *Bull. Mar. Sci.*, **27**, 256–291.

Deuser, W. G., Ross, E. H. and Anderson, R. F. (1981) Seasonality in the supply of sediment to the deep Sargasso Sea and implications for the rapid transfer of matter to the deep ocean. *Deep-Sea Res.*, **28**, 495–505.

Dickey, T., Zedler, S., Yu, X. *et al.* (2001) Physical and biogeochemical variability from hours to years at the Bermuda Testbed Mooring site: June 1994-March 1998. *Deep-Sea Res. II*, **48**, 2105–2140.

Eden, B. R., Steinberg, D. K., Goldthwait, S. A. *et al.* (2009) Zooplankton community structure in anticyclonic and mode-water eddy in the Sargasso Sea. *Deep-Sea Res. I*, **56**, 1757–1776.

Fang, J., Conte, M. H. and Weber, J. C. (2010) Influence of physical forcing on seasonality of biological components and deep ocean particulate flux in the Sargasso Sea. *Eos Trans. AGU, 91(26), Ocean Sci. Meet. Suppl.*, Abst. BO24B-02.

Fowler, S. W. and Knauer, G. A. (1986) Role of large particles in transport of elements and organic compounds through the oceanic water column. *Prog. Oceanogr.*, **16**, 147–194.

Goldthwait, S. A. and Steinberg, D. K. (2008) Elevated biomass of mesozooplankton and enhanced fecal pellet flux in cold core and mode water eddies in the Sargasso Sea. *Deep-Sea Res. II*, **55**, 1360–1377.

Gonzalez, E. G. and Smetacek, V. (1994) The possible role of the cyclopoid copepod *Oithona* in retarding vertical flux of zooplankton faecal material. *Mar. Ecol. Prog. Ser.*, **113**, 233–246.

Gonzalez, H. E., Gonzalez, S. R. and Brummer, G.-J. A. (1994) Short-term sedimentation pattern of zooplankton, faeces and microplankton at a permanent station in the Bjarnafjorden (Norway) during April-May 1992. *Mar. Ecol. Prog. Ser.*, **105**, 31–45.

Gonzalez, H. E., Hebbeln, D., Iriarte, J. L. *et al.* (2004) Downward fluxes of faecal material and microplankton at 2300 m depth in the oceanic area off Coquimbo (30 degrees S), Chile, during 1993–1995. *Deep-Sea Res. II*, **51**, 2457–2474.

Gonzalez, H. E., Ortiz, V. C. and Sobrazo, M. (2000) The role of the faecal material in the particulate organic matter flux in the northern Humbolt Current, Chile (23^0 S), before and during the 1997–1998 El Nino. *J. Plankton Res.*, **22**, 499–529.

Gooday, A. J. (2002) Biological responses to seasonally varying fluxes of organic matter to the ocean floor: a review. *J. Oceanogr.*, **58**, 305–332.

Gowing, M. M., Garrison, D. L., Kunze, H. B. *et al.* (2001) Biological components of Ross Sea short-term particle fluxes in the austral summer of 1995–1996. *Deep-Sea Res*, **48**, 2645–2671.

Hernández-León, S., Almeida, C., Gómez, M. *et al.* (2001) Zooplankton biomass and indices of feeding and metabolism in island-generated eddies around Gran Canaria. *J. Mar. Sys.*, **30**, 51–66.

Honjo, S., Manganini, S. J., Krishfield, R. A. *et al.* (2008) Particulate organic carbon fluxes to the ocean interior and factors controlling the biological pump: a synthesis of global sediment trap programs since 1983. *Progr. Oceanogr.*, **76**, 217–285.

Huang, S. and Conte, M. (2009) Source/process apportionment of major and trace elements in sinking particles in the Sargasso Sea. *Geochim. Cosmochim. Acta*, **73**, 65–90.

Huskin, I., Viesca, L. and Anadon, R. (2004) Particle flux in the Subtropical Atlantic near the Azores: influence of mesozooplankton. *J. Plankton Res.*, **26**, 403–415.

Jackson, G. A. and Checkley, D. M. (2011) Particle size distributions in the upper 100 m water column and their implications for animal feeding in the plankton. *Deep Sea Res. I*, **58**, 283–297.

Jiang, S., Dickey, T., Steinberg, D. *et al.* (2007) Temporal variability of zooplankton biomass from ADCP backscatter time series data at the Bermuda Test Bed Mooring Site, *Deep Sea Res. I*, **54**, 608–636.

Krause, J. W., Nelson, D. M. and Lomas, M. W. (2010) Production, dissolution, accumulation and potential export of biogenic silica in a Sargasso Sea mode-water eddy. *Limnol. Oceanogr.*, **55**, 569–579.

Labat, J-P., Gasparini, S., Mousseau, L. *et al.* (2009) Mesoscale distribution of zooplankton biomass in the northeast Atlantic Ocean determined with an Optical Plankton Counter: relationship with environmental structures. *Deep-Sea Res. I*, **56**, 1742–1756.

Lampitt, R. S. and Antia, A. N. (1997) Particle flux in deep seas: regional characteristics and temporal variability. *Deep-Sea Res. I*, **44**, 1377–1403.

Lampitt, R. S., Noji, T. T. and von Bodungen, B. (1990) What happens to zooplankton faecal pellets? Implications for material flux. *Mar. Biol.*, **104**, 15–23.

Landry, M. R., Decima, M., Simmons, M. P. *et al.* (2008) Mesoscale biomass and grazing responses to Cyclone Opal, a subtropical mesoscale eddy. *Deep-Sea Res. II*, **55**, 1378–1388.

Ledwell, J. R., McGillicuddy, D. J. and Anderson, L. A. (2008) Nutrient influx into intense deep chlorophyll layer in a mode-water eddy. *Deep-Sea Res. II*, **55**, 1139–1160.

Mackas, D. L., Tsurumi, M., Galbraith, M. D. *et al.* (2005) Zooplankton distribution and dynamics in a North Pacific Eddy of coastal origin: II. Mechanisms of eddy colonization by and retention of offshore species. *Deep-Sea Res. II*, **52**, 1011–1035.

Madin, L. P., Horgan, E. F. and Steinberg, D. K. (2001) Zooplankton at the Bermuda Atlantic Time-series Study (BATS) station: diel, seasonal and interannual variation in biomass, 1994–1998. *Deep-Sea Res. II*, **48**, 2063–2082.

McGillicuddy, D. J., Johnson, R., Siegel, D. A. *et al.* (1999) Mesoscale variations of biogeochemical properties in the Sargasso Sea. *J. Geophys. Res.*, **104**, 13381–13394.

McGillicuddy, D. J. and Robinson, A. R. (1997) Eddy-induced nutrient supply and new production in the Sargasso Sea. *Deep-Sea Res. I*, **44**, 1427–1450.

Michaels, A. F. and Knap, A. H. (1996) Overview of the U.S. JGOFS BATS and Hydrostation S program. *Deep-Sea Res.*, **43**, 157–198.

Miquel, J. C., Fowler, S. W., La Rosa, J. *et al.* (1994) Dynamics of the downward flux of particles and carbon in the open northwestern Mediterranean Sea. *Deep Sea Res. I*, **41**, 243–261.

Noji, T. T., Estep, K. W., MacIntyre, F. *et al.* (1991) Image analysis of fecal material grazed upon by three species of copepods. Evidence for coprohexy, coprophagy and coprochaly. *J. Mar. Biol. Assoc. U.K.*, **71**, 465–480.

Pilskaln, C. H. and Honjo, S. (1987) The fecal pellet fraction of the biogeochemical particle fluxes to the deep sea. *Global Biogeochem. Cycles*, **1**, 31–48.

Ploug, H., Iversen, M. H. and Fischer, G. (2008) Ballast, sinking velocity, and apparent diffusivity within marine snow and zooplankton fecal pellets: implications for substrate turnover by attached bacteria. *Limnol. Oceanogr.*, **53**, 1878–1886.

Roman, M. R., Caron, D. A., Kremer, P. *et al.* (1995) Spatial and temporal changes in the partitioning of organic carbon in the plankton community of the Sargasso Sea off Bermuda. *Deep-Sea Res. I*, **42**, 973–992.

Siegel, D. A. and Armstrong, R. A. (2002) Corrigendum to "Trajectories of sinking particles in the Sargasso Sea: modeling of statistical funnels above deep-ocean sediment traps". *Deep-Sea Res. I*, **49**, 1115–1116.

Siegel, D. A., McGillicuddy, D. J. and Fields, E. A. (1999) Mesoscale eddies, satellite altimetry, and new production in the Sargasso Sea. *J. Geophys. Res.*, **104**, 13359–13379.

Small, L. F., Fowler, S. W. and Unlu, M. Y. (1979) Sinking rates of natural copepod fecal pellets. *Mar. Biol.*, **51**, 233–241.

Smetacek, V. (1980) Zooplankton standing stock, copepod faecal pellets and particulate detritus in Kiel Bight. *Estuar. Coat. Mar. Sci.*, **11**, 477–490.

Smeti, H. E., Jiang, S., Conte, M. H. *et al.* (2010) Mesoscale eddies enhance macrozooplankton abundance and carbon export to the deep ocean in the northwestern Sargasso Sea. *Eos Trans. AGU, 91(26), Ocean Sci. Meet. Suppl.*, Abst. BO25G-16.

Smith, W. O. Jr., Shields, A. R., Dreyer, J. C. *et al.* (2011) Interannual variability in vertical export in the Ross Sea: magnitude, composition, and environmental correlates. *Deep-Sea Res. I*, **58**, 147–159.

Steinberg, D. K., Carlson, C. A., Bates, N. R. *et al.* (2001) Overview of the US JGOFS Bermuda Atlantic Time-series Study (BATS): a decade look at ocean biology and biogeochemistry. *Deep-Sea Res. II*, **48**, 1405–1447.

Strzelecki, J., Koslow, J. A. and Waite, A. (2007) Comparison of mesozooplankton communities from a pair of warm- and -cold-core eddies off the coast of Western Australia. *Deep-Sea Res. II*, **54**, 1103–1112.

Sweeny, E. N., McGillicuddy, D. J. and Buesseler, K. O. (2003) Biogeochemical impacts due to mesoscale eddy activity in the Sargasso Sea as measured at the Bermuda Atlantic Time-series Study (BATS). *Deep-Sea Res. II*, **50**, 3017–3039.

Taylor, G. T. (1989) variability in the vertical flux of microorganisms and biogenic material in the epipelagic zone of a North pacific central gyre station. *Deep-Sea Res.*, **36**, 1287–1308.

Turner, J. T. (2002) Zooplankton fecal pellets, marine snow and sinking phytoplankton blooms. *Aquat. Microb. Ecol.*, **27**, 57–102.

Urban-Rich, J., Hansell, D. A. and Roman, M. R. (1998) Analysis of copepod fecal pellet carbon using a high temperature combustion method. *Mar. Ecol. Prog. Ser.*, **171**, 199–208.

Urrère, M. A. and Knauer, G. A. (1981) Zooplankton fecal pellet fluxes and vertical transport of particulate organic material in the pelagic environment. *J. Plankton Res.*, **3**, 369–387.

Uye, S. and Kaname, K. (1994) Relations between fecal pellet volume and body size for major zooplankters of the inland Sea of Japan. *J. Oceanogr.*, **50**, 43–49.

Wassmann, P. (1998) Retention versus export food chains: processes controlling sinking loss from marine pelagic systems. *Hydrobiologia*, **363**, 29–57.

Wassmann, P., Ypma, J. E. and Tselepides, A. (2000) Vertical flux of faecal pellets and microplankton on the shelf of the oligotrophic Cretan Sea (NE Mediterranean Sea). *Progr. Oceanogr.*, **46**, 241–258.

Wexels Riser, C., Wassmann, P., Olli, K. *et al.* (2001) Production, retention and export of zooplankton faecal pellets on and off the Iberian shelf, north-west Spain. *Prog. Oceanogr.*, **51**, 423–442.

Wexels Riser, C., Wassmann, P., Olli, K. *et al.* (2002) Seasonal variation in production, retention and export of zooplankton faecal pellets in the marginal ice zone and central Barents Sea. *J. Mar. Systems*, **38**, 175–188.

Wexels Riser, C., Wassmann, P., Reigstad, M. *et al.* (2008) Vertical flux regulation by zooplankton in the northern Barents Sea during Arctic spring. *Deep-Sea Res. II*, **55**, 2320–2329.

Wilson, S. E., Steinberg, D. K. and Buesseler, K. O. (2008) Changes in fecal pellet characteristics with depth as indicators of zooplankton repackaging of particles in the mesopelagic zone of the subtropical and subarctic North Pacific Ocean. *Deep-Sea Res. II*, **55**, 1636–1647.

Yamaguchi, A., Watanabea, Y., Ishidaa, H. *et al.* (2002) Community and trophic structures of pelagic copepods down to greater depths in the western subarctic Pacific (WEST-COSMIC). *Deep-Sea Res. I*, **49**, 1007–1025.

Yebra, L., Almeida, C. and Hèrnandez-León, S. (2005) Vertical distribution of zooplankton and active flux across and anticyclonic eddy in the Canary Island waters. *Deep-Sea Res. I*, **52**, 68–93.

Yebra, L., Hèrnandez-León, S., Almeida, C. *et al.* (2004) The effect of upwelling filaments and island induced eddies on induces of feeding, respiration and growth in copepods. *Prog. Oceanogr.*, **62**, 151–169.

Youngbluth, M. J., Bailey, T. G., Davoll, P. J. *et al.* (1989) Fecal pellet production and diel migratory behavior by the euphausiid *Medanyctiphanes norvegica* effect benthic-pelagic coupling. *Deep-Sea Res.*, **36**, 1491–1501.